THERMOELASTICITY OF LARGE LECITHIN BILAYER VESICLES

RON KWOK and EVAN EVANS, *Department of Pathology, University of British Columbia, Vancouver, British Columbia, Canada V6T 1W5*

ABSTRACT Micromechanical experiments on large lecithin bilayer vesicles as a function of temperature have demonstrated an essential feature of bilayer vesicles as closed systems: the bilayer can exist in a tension-free state (within the limits of experimental resolution, i.e., $<10^{-2}$ dyn/cm). Furthermore, because of the fixed internal volume, there is a critical temperature at which the vesicle becomes a tension-free sphere. Below this temperature, thermoelastic tension builds up in the membrane and the vesicle's internal pressure increases while the surface area remains constant. Above this temperature, the vesicle's surface area increases while the tension and internal pressure are negligible. Without mechanical support, the vesicles fragment into smaller vesicles because they have insufficient surface rigidity. In the upper temperature range we have measured the increase of surface area with temperature. These data established the thermal area expansivity to be 2.4×10^{-3}/°C. At constant temperature, we used either pipet aspiration with suction pressures up to 10^4 dyn/cm^2 or compression against a flat surface with forces up to 10^{-2} dyn to produce area dilation of the vesicle surface on the order of 1%. The rate of increase of membrane tension with area dilation was calculated, which established the elastic area compressibility modulus to be 140 dyn/cm. The tension limit that produced lysis was observed to be 3–4 dyn/cm (equivalent to 2–3% area increase). The product of the elastic area compressibility modulus, the thermal area expansivity, and the temperature gives the reversible heat of expansion at constant temperature for the bilayer. This value is 100 ergs/cm^2 at 25°C, or ~5 kcal/mol of lecithin. Similarly, the product of the thermal area expansivity multiplied by the area compressibility modulus determines the rate of increase of thermoelastic tension with decrease in temperature when the area is held constant, i.e., −0.34 dyn/cm/°C.

INTRODUCTION

Phospholipid bilayers are integral components of the thin membranes that encapsulate cellular organisms. The lamellar configuration of phospholipids is the result of the preferential assembly of the amphiphilic molecules whose acyl chains are located interior to the bilayer and whose polar head groups are anchored to the aqueous interfaces. Because of the strong preference for the bilayer arrangement, the encapsulating membrane of a biological cell or artificial lipid vesicle behaves as a closed system for periods of time on the order of hours. Since there is no exchange of material, mechanical experiments can be used to investigate the state of the membrane *in situ*.

Phospholipid bilayer membranes above the order-disorder phase transition temperature for the acyl chains behave as surface-isotropic liquids. Hence, their surface elasticity is characterized by a single isothermal constitutive relation between the bilayer isotropic tension, $\bar{T}$, and the fractional change in surface area, α, of the bilayer (see Evans and Skalak, 1979 or 1980, for an outline of membrane mechanical properties). The proportionality factor in this relation

is the elastic area compressibility modulus, K, at constant temperature. Previously, no direct mechanical experiments have been performed on solvent-free bilayer membranes, although research has been done on bilayer films that contain organic solvents; e.g., measurement of surface tension in spherical films (Tien, 1967; Pagano and Thompson 1973), and electrocompression of planar lipid films (Crowley, 1973; White and Thompson 1973; Requena et al., 1975; Alvarez and Latorre, 1978). Surface elastic properties have also been deduced from analysis of dehydration of multilamellar lipid/water phases combined with x-ray diffraction data (Parsegian et al., 1979; Evans and Skalak, 1979). In early bilayer film measurements, the tensions were totally dominated by the free exchange of lipids and solvent with lenses and peripheral boundaries. Subsequent experiments (e.g., Alvarez and Latorre, 1978) minimized the exchange with the use Montal and Mueller's (1972) technique of bilayer film formation. This experiment, however, is still vulnerable to lipid exchange at the boundaries, especially when subjected to thickness compression. Recently, we have developed experimental techniques to measure thermoelastic properties of large phospholipid bilayer vesicles directly.

In contrast to lipid bilayer membranes, the mechanical properties of red blood cell membranes have been studied extensively (see Evans and Hochmuth, 1978, for a review of the literature). Measurements have shown that the red cell membrane resistance to area dilation is more than four orders of magnitude greater than its resistance to extensional (shear) deformations of the surface (Evans et al. 1976; Evans and Waugh, 1977*b;* Waugh and Evans, 1979). At 25°C, the measured values of the elastic area compressibility modulus and surface shear modulus of the red cell membrane are 450 dyn/cm and 6.6×10^{-3} dyn/cm, respectively. Thermoelastic experiments showed that the fractional change in membrane area with temperature is 1.3×10^{-3}/°C and that the reversible heat of expansion of the red cell surface varied between 200 and 100 ergs/cm^2 for the temperature range of 2–50°C. On the other hand, the reversible heat of surface extension was found to be only 2×10^{-2} ergs/cm^2. These data demonstrate that the strong cohesive interactions in the membrane surface are surface-isotropic, i.e. "liquid-like" in character.

In this article we present experimental results for mechanical deformation of large (diameter $>10^{-3}$ cm) egg lecithin bilayer vesicles. From these data we derive the mechanical state and surface elastic properties for a lecithin bilayer as a single component, closed membrane material. Specifically, we determine the bilayer tension in the unstressed state and the increase in tension which is produced by mechanical deformation of the vesicle. We also determine the fractional increase in surface area of the unstressed vesicle with increase in temperature (i.e., the thermal area expansivity); combined with the mechanical deformation data, the thermal area expansivity yields the reversible heat of expansion for the lecithin bilayer surface.

EXPERIMENTAL METHODS

The procedure for preparation of large phospholipid vesicles was adapted from that of Reeves and Dowben (1969). First, ~0.1 ml of lipid mixture (which is dissolved in 10:1 chloroform-methanol at a concentration of 100 mg/ml) was added to a small glass tube. The solvent was evaporated by passing argon gas over the sample. Residual solvent was removed by placing the sample in vacuo for 24 h. 15 ml of buffer was then added to the sample and the sample was allowed to swell at 45°C for 1 h. Finally, the dispersion was swirled gently and centrifuged at 10,000 rpm for 15 min to remove undispersed lipids. The supernate was used for the vesicle experiments.

We used two different mechanical techniques to measure the vesicle membrane elastic properties: micropipet aspiration and compression between a micropipet and a thin platinum beam (force-transducer). For both tests, vesicles were injected (in very weak concentration) into a microchamber (1 × 2 × 0.1 cm), which was mounted on the stage of an inverted microscope. The chamber temperature was controlled to 0.1°C over a range of 2–60°C and was monitored by a small thermocouple in the microchamber itself. A long working length objective was used to avoid heat conduction from the

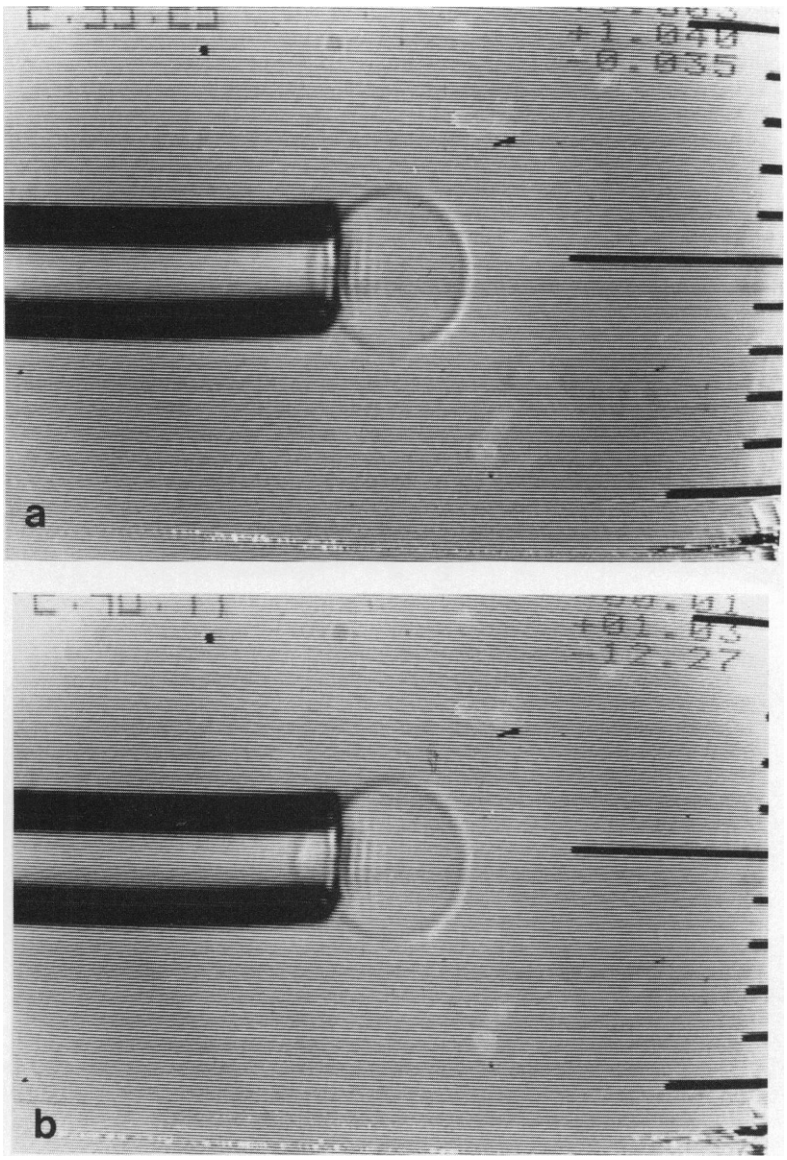

FIGURE 1 Video recordings of micropipet aspiration of a large lecithin bilayer vesicle. The displacement of the projection in the pipet is proportional to the area dilation. The suction pressures are 35 dyn/cm^2 and 12,270 dyn/cm^2 for the conditions in (*a*) and (*b*) respectively. The vesicle wall is only ~40 × 10^{-8} cm thick, whereas the vesicle diameter is ~15 × 10^{-4} cm. The image is enhanced by a Hoffman phase optical system.

chamber. Temperature, pressures, and time were simultaneously recorded on video tape with video multiplexing. A micrometer eyepiece was always in the video microscope image in order that the system could be calibrated at the time of recording. A Hoffman phase optical system was used to enhance the vesicle image. Glass micropipets ($1–10 \times 10^{-4}$ cm i.d.) were pulled from 0.1-cm glass tubing to a needle point and then broken by quick fracture to the desired tip diameter. Accurate measurement of the tip inner diameter was obtained from the insertion depth of a tapered microneedle, which was calibrated with a scanning electron microscope.

The micropipet suction test called for aspiration of a large vesicle ($\sim 2 \times 10^{-3}$ cm diameter) with a small pipet ($\sim 8–10 \times 10^{-4}$ cm i.d.). The suction pressures ranged from 10 to 10^4 dyn/cm^2. Because of the ionic strength ($\sim$0.1 mol NaCl) of the suspending buffer, the internal volume of a vesicle remained nearly constant when the vesicle was aspirated (see Appendix A). Hence, the displacement of the vesicle projection inside the pipet was proportional to the change in area of the vesicle. Fig. 1 shows videorecorded images of a micropipet suction test.

In the beam compression test, a vesicle was held with a fixed suction pressure by a thickwalled pipet of small inner diameter. The vesicle was then compressed against a thin platinum beam ($\sim 3–4 \times 10^{-4}$ cm thick). The deflection of the beam provided the measure of total compression force. The method of calibration is described by Evans et al. (1980). The increase in equatorial radius is a direct (but not linear) function of the increase in vesicle surface area. Fig. 2 shows a videorecorded image of a beam compression test.

The thermal area expansion tests were performed at negligible stress levels (either suction pressure or beam force). The temperature was increased and either the displacement of the projection inside the pipet or the change in equatorial radius was observed to obtain the area increase.

Both mechanical tests gave the same results within the experimental error. We will treat the micropipet aspiration experiment in the sections that follow because it involves a simpler analysis.

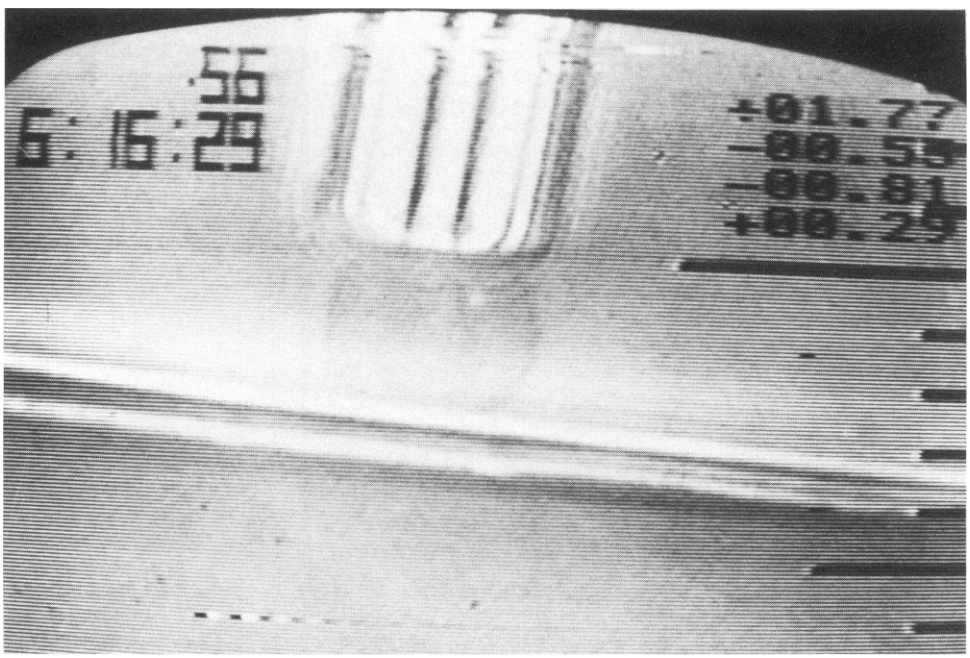

FIGURE 2 Video recording of compression of a large lecithin vesicle ($\sim 20 \times 10^{-4}$ cm diameter) against a thin platinum beam ($\sim 3 \times 10^{-4}$ cm thick). The beam deflection is the measure of total compression force. The image is modified by Zernicke phase contrast.

Appendix B contains a brief outline of the beam compression test. Further details on methods are given by Kwok (1980).

RESULTS AND ANALYSIS

In the micropipet suction test, the projection of the vesicle inside the pipet may be increased by two independent processes: (*a*) the temperature is increased with the suction pressure held constant, and (*b*) the suction pressure is increased with the temperature held constant. Both processes are observed to be reversible. The increase in projection length, L, is simply related to small changes in vesicle surface area, A, and volume, V, by

$$\Delta A \simeq \pi \left[D_p \cdot \Delta L \cdot (1 - D_p/D_c) + \frac{4\Delta V}{\pi D_c} \right], \tag{1}$$

where D_p is the pipet diameter, and D_c is the diameter of the spherical portion of the vesicle outside the pipet. As noted previously and in Appendix A, the change in volume is negligible. Thus, the displacement of the vesicle projection inside the pipet is proportional to the change in vesicle surface area.

For the first process, Fig. 3 shows the surface area of a particular vesicle as a function of temperature. It is significant that there is a critical temperature, T_c, where the vesicle is exactly a sphere. Since the volume is fixed, the area cannot decrease below this temperture and the vesicle remains spherical. Nonetheless, the initial membrane tension in the sphere increases in proportion to the reduction in temperature below T_c. Above T_c, the initial membrane tension is imperceptible (i.e., it takes very small suction pressures to aspirate the vesicle initially; see Fig. 1*a*, for example). The vesicle surface area increases with temperature

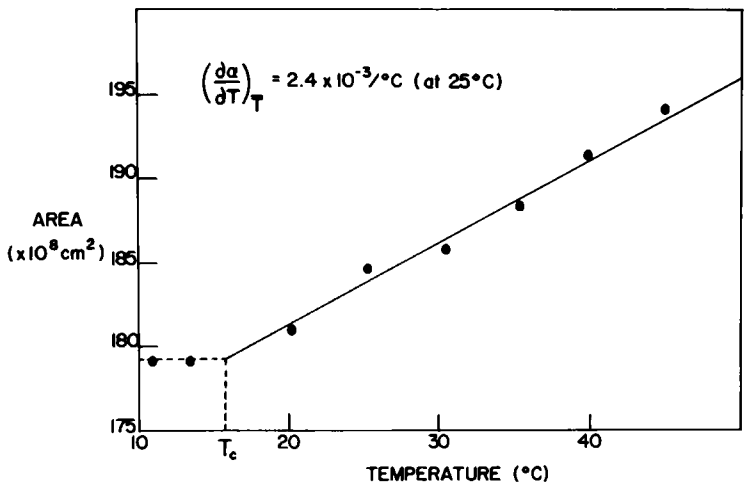

FIGURE 3 Data for the area of a large lecithin vesicle as a function of temperature. The temperature T_c is the critical value where the vesicle is an unstressed sphere. Above T_c, the area increases with temperature (stress-free); below T_c, the area is constant but the membrane tension increases as the temperature is reduced. The thermal area expansivity is the fractional rate of increase in area with increase in temperature, 2.4 × 10^{-3}/°C. The dashed line is the temperature range where the vesicle is a sphere with constant area and volume.

above T_c and creates a "flaccid" capsule. If the area excess (above the critical value for a sphere of equal volume) is too great, the vesicle will break up into smaller fragments unless it is supported by rigid boundaries because it lacks surface shear rigidity. The critical temperature, T_c, is variable and depends on the preparation history of the vesicle formation.

The observed dependence of surface area on temperature is a consequence of the "closed" surface of the vesicle (Evans and Waugh, 1977a). The slope of the area increase above T_c yields the thermal area expansivity for the membrane, at zero tension,

$$\left(\frac{\partial \alpha}{\partial T}\right) = \frac{1}{A_0}\left(\frac{\partial A}{\partial T}\right),$$

where A_0 is the vesicle area at a reference state and T is temperature. The results for 31 vesicles are summarized in Fig. 4, with an average value of 2.4×10^{-3}/°C. Similar results obtained in the vesicle compression experiments are discussed in Appendix B.

In contrast to the area expansion of the vesicle with increase in temperature, the area expansion produced by membrane tension depends on the number of bilayers that makeup the vesicle membrane. In other words, the more bilayers there are, the greater the elastic resistance to area dilation. To minimize the number of layers, we selected vesicles that by observation appeared the most transparent. Within this group, we could differentiate between single and multiwalled vesicles because the elastic moduli separated into groups that were almost integral multiples. The lowest group was chosen to represent single bilayer vesicles.

Figure 5*a* shows the pipet suction pressure vs. vesicle projection length for a single vesicle aspiration above T_c. Figure 5*b* is a ×30 enlargement of the pressure scale in Fig. 5*a* to show the very small pressures required to aspirate the vesicle initially. The initial pressures (~30–50 dyn/cm^2) correspond to membrane tensions of $< 10^{-2}$ dyn/cm, which are more than two orders of magnitude smaller than the subsequent tensions required to produce 1–2% area

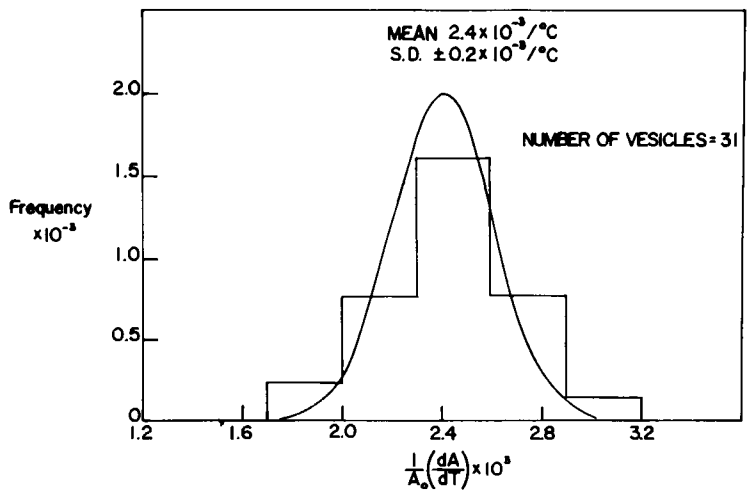

FIGURE 4 Histogram of thermal area expansivity from micropipet aspiration experiments on large lecithin vesicles. The average is determined to be 2.4×10^{-3}/°C. A normal distribution function has been superimposed with the mean and standard deviation of the data.

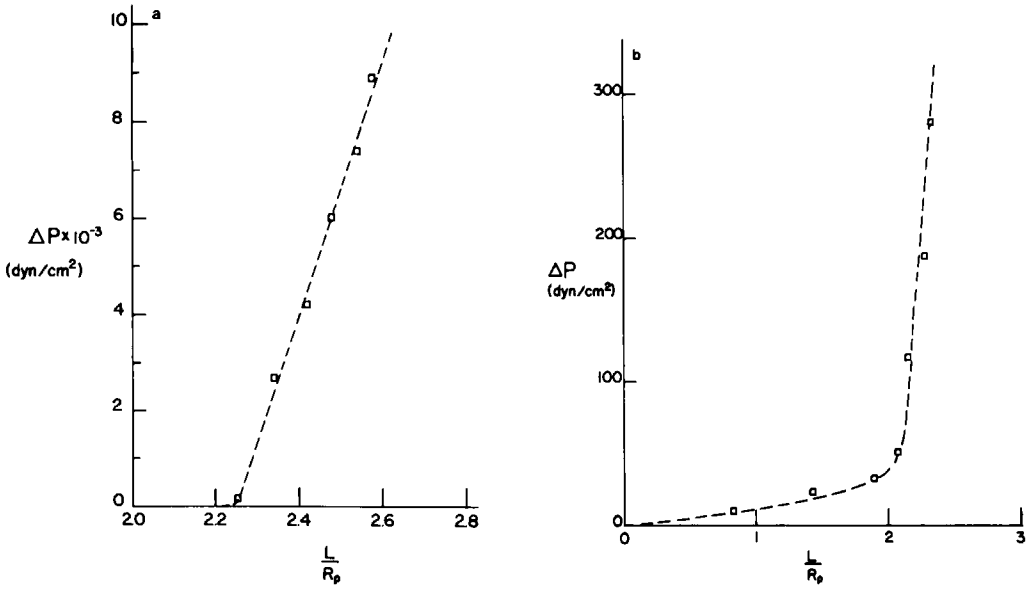

FIGURE 5 Data for the pipet suction pressure vs. length of the vesicle projection inside the pipet. The pressure data for this single vesicle experiment is presented on two scales to illustrate (*a*) the linear relation of suction pressure to aspiration length in the range where the surface area is forced to dilate, and (*b*) the very small pressures initially required to aspirate the vesicle. The initial pressures correspond to membrane tension levels $< 10^{-2}$ dyn/cm; the subsequent pressures that dilate the surface correspond to tensions >1 dyn/cm.

dilation. The initial pressure range appears to be due to curvature elastic (bending) rigidity of the membrane. The level of suction pressure associated with membrane bending is on the order of $\Delta P \sim 2B/(R_c^2 \cdot D_p)$ (see Appendix C), where B is the bending modulus and R_c is the radius of curvature for the bend at the edge of the pipet entrance (Evans and Sklak, 1979). Estimates of bilayer bending moduli are in the range of 10^{-13}–10^{-12} dyn-cm (Evans and Hochmuth, 1978); hence, with a radius of curvature of 10^{-5} cm at the bend, the initial pressure range would be 10–10^2 dyn/cm^2, which is comparable to the observed values. We are presently analyzing the membrane bending in order to derive the bending modulus from this initial aspiration data.

As Fig. 5*a* demonstrates, the suction pressure exhibits a linear dependence on the projection length as the vesicle area is expanded. At mechanical equilibrium the isotropic tension is constant over the entire surface (except in the sharp bend at the pipet entrance, Appendix C) and is simply proportional to the suction pressure, ΔP:

$$4\bar{T} = D_p \cdot \Delta P/(1 - D_p/D_c). \tag{2}$$

Therefore, the isotropic tension may be expressed by an elastic constitutive relation in terms of the fractional area dilation, $\alpha \equiv \Delta A/A_0$:

$$\bar{T} = \bar{T}_0 + K\alpha, \tag{3}$$

where K is the isothermal elastic area compressibility modulus, and $\bar{T}_0$ is the initial tension. In

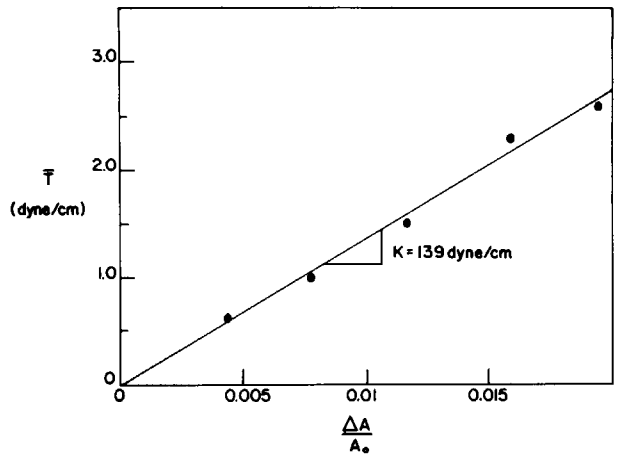

FIGURE 6 Membrane tension vs. the fractional area dilation of a single-walled lecithin vesicle derived from the previous pressure-length data. The solid curve is the linear correlation based on the area compressibility modulus of 139 dyn/cm.

the range of temperatures where the vesicle is flaccid, $\bar{T}_0$ is negligible. Below the critical temperature, the values of initial tension would range from 0 to ~3 dyn/cm at the temperature where the vesicle lyses. As we shall see later, the initial tension in this lower range is a thermoelastic stress.

Fig. 6 is the membrane tension vs. the fractional area dilation calculated from the data in Fig. 5*a*. The slope of the linear correlation is the elastic area compressibility modulus. Fig. 7 shows the cumulated results for 35 vesicle tests. The moduli separate into two groups (more rigid vesicles are occasionally observed but are difficult to analyze). The lowest group is taken

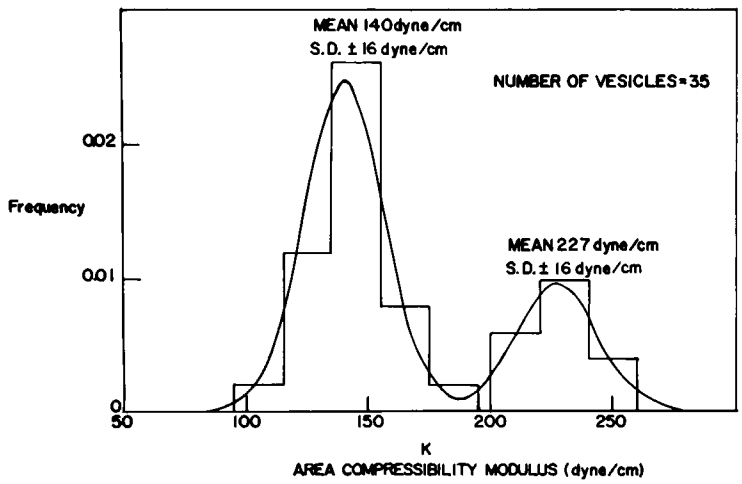

FIGURE 7 Histogram of elastic area compressibility moduli from micropipet aspiration experiments on large lecithin vesicles. The results group according to the number of bilayer walls in the vesicles: lowest group is single-walled; next group is double-walled. Two independent, normal distribution functions have been superimposed with the mean values and standard deviations of the data group.

as the single bilayer vesicle population with an average modulus of 140 dyn/cm. Two independent, normal distribution functions have been correlated with each group and then superimposed on the results in Fig. 7. Similar results obtained in the beam compression experiments are presented in Fig. A3 of Appendix B.

These experiments provide data for decomposition of membrane thermodynamic potential changes into internal energy and configurational entropy contributions (Evans and Waugh, 1977*a*). For a reversible (elastic) process, the differential work is related to the combined first and second laws of thermodynamics, $d\tilde{W} = d\tilde{E} - Td\tilde{S}$, where $\tilde{E}$ is the internal energy density (ergs/cm^2) of the membrane, and $\tilde{S}$ is the entropy density (ergs/cm^2/°C) of the membrane material. Cross derivatives plus differential expressions for the thermodynamic state functions, $\tilde{E}$ and $\tilde{S}$, relate the partial derivatives of internal energy density and entropy density to coefficients in the membrane equations of state. The reversible heat of expansion is

$$T\left(\frac{\partial \tilde{S}}{\partial \alpha}\right)_T = TK\left(\frac{\partial \alpha}{\partial T}\right). \tag{4}$$

When the membrane isotropic tension is zero, the free energy density at constant temperature is a minimum with respect to variations in area:

$$\left(\frac{\partial \tilde{E}}{\partial \alpha}\right)_T - T\left(\frac{\partial \tilde{S}}{\partial \alpha}\right)_T = 0.$$

The heat of expansion at zero tension, $TK\ (\partial\alpha/\partial T)$, is opposed by the increase in internal energy density with expansion. Hence, the heat of expansion is interpreted as a measure of membrane cohesion. With the data just described for (egg) lecithin, the reversible heat of expansion is 100 ergs/cm^2, equivalent to 5 kcal/mol of lecithin, at 25°C. The value of the reversible heat of expansion is about twice the free energy of exposure of hydrocarbon to water.

The thermoelastic relation for the change in tension with temperature at *fixed* membrane area is derived from the reversible heat of expansion (Evans and Waugh, 1977*a*),

$$\left(\frac{\partial \bar{T}}{\partial T}\right)_{\alpha=0} = -K\left(\frac{\partial \alpha}{\partial T}\right). \tag{5}$$

This equation describes the increases of membrane tension for the vesicle as a sphere of fixed volume and area in proportion to the temperature reduction below T_c. On the basis of the previous results, Eq. 5 predicts that the initial membrane tension will increase by 0.34 dyn/cm as the temperature is lowered by each degree. It was observed experimentally that the temperature reduction which caused vesicles to lyse was ~10°C. Hence, the membrane thermoelastic tension at lysis is calculated to be ~3 dyn/cm. This value is comparable to the level of membrane tension which produced lysis of flaccid vesicles with pipet suction above T_c.

SUMMARY AND DISCUSSION

In summary, we have used two different micromechanical tests to measure thermoelastic properties of a single bilayer membrane in the form of a large vesicle. These experiments have

shown that a vesicle bilayer can exist in a tension-free state ($<10^{-2}$ dyn/cm). At constant temperature, the elastic resistance to area dilation is given by an average modulus of 140 dyn/cm for a single bilayer. In the tension-free state, the average fractional increase in membrane area is 2.4×10^{-3} per degree temperature increase. With these data, the thermoelastic relation predicts that the bilayer tension would increase by 0.34 dyn/cm per degree temperature decrease for a spherical vesicle with constant surface area and internal volume. Likewise, the reversible heat of expansion is calculated to be 100 ergs/cm^2 (5 kcal/mol of lecithin) at 25°C. How do these results compare with previous experiments?

As we noted in the introduction, early bilayer film measurements exhibited open system behavior that involved exchange of material with peripheral boundaries and lenses. The experimental work of Alvarez and Latorre (1978) is the best work in this regard since little exchange was possible. Their data yielded a modulus for electrocompressive stress vs. fractional change in thickness on the order of 10^9 dyn/cm.[2] With the thickness of 3×10^{-7} cm derived from the capacitance measurements, the equivalent area modulus would be 300 dyn/cm. Their calculation assumes that the film area is able to increase, but because of the rigid support boundaries, the amphiphiles were probably forced out of the film onto the support. In this case, the value would be a factor of two lower, 150 dyn/cm, which would closely agree with our results.

The reversible extraction of water (i.e., dehydration) from multilamellar lipid/water phases has been shown to change reversibly the area per lipid molecule (Reiss-Husson, 1967). The careful experiments of LeNeveu et al. (1977) and Parsegian et al. (1979) have determined the work required to extract water from the multilamellar system as a function of water content and the bilayer repeat spacing in a multilamellar phase. The water fraction and repeat spacing data are combined to give mass-average bilayer and water layer thicknesses. The area-per-molecule values are calculated from the volumes per lipid molecule divided by the half-bilayer thickness. The work per molar volume of water extracted is equal to the osmotic stress supported by the multilamellar system (LeNeveu et al., 1977). The osmotic stress (which is a reduced pressure in the water gap between bilayers) is opposed by the repulsion across the water gap and by a compressive force resultant (negative tension) in the bilayer plane. This is analogous to the extraction of water from an elastic "sponge." Consequently, it is possible to determine the relationship between the compressive force resultant and area per molecule in the bilayer from the osmotic stress and multilamellar geometry (Parsegian et al., 1979; Evans and Skalak, 1979). We expect that the elastic constitutive relation, Eq. 3, should be continuous from tension to compression. With an area compressibility modulus of 140 dyn/cm, the agreement is good for area-per-molecule values < 67 Å^2. Above 67 Å^2, up to 75 Å^2, the apparent area compressibility modulus is at least an order of magnitude lower as calculated from the data of Parsegian et al. (1979). Thus, our results indicate that the unstressed area per molecule would have to be 66–68 Å^2 in order for the elastic behavior to be continuous from our tension experiments to their compression experiments.

There have also been x-ray diffraction measurements as a function of temperature on multibilayer systems at fixed water content. From these experiments, the fractional decrease in thickness as a function of increase in temperature has been derived. The thermal thickness expansivity was determined to be -2×10^{-3}/°C by Rand and Pangborn (1973). The thermal area expansivity is the thermal volume expansivity minus the thermal thickness expansivity.

Thus, the thermal area expansivity is larger than the thermal thickness expansivity. Although no measurements have been made of thermal volume expansivity with egg lecithin, results for saturated chain lipids (Nagel and Wilkinson, 1978; McDonald, 1978) indicate a value of 4–5 $\times 10^{-4}/°C$. Therefore the x-ray measurements agree well with the thermal area expansivity which we have measured, i.e., $2.4 \times 10^{-3}°C$.

APPENDIX A

If the volume changes with pipet suction pressure, then the area change must be corrected for the change in volume in Eq. 1. Since the volume change is too small to measure directly, mass transport equations are used to model the osmotic equilibrium for the vesicle in order to calculate the volume change. The critical assumptions in the analysis are: (*a*) the permeability of water is uniform and constant over the vesicle surface, (*b*) negligible transport of water occurs where the membrane is adjacent to the pipet wall (i.e., the cylindrical section of the vesicle projection in the pipet), and (*c*) the flux of water out of the vesicle is given by a linear transport equation. With this approach and the equations of mechanical equilibrium, a simple relation is obtained for the fractional change in volume of the vesicle as a function of membrane tension and vesicle solute concentration, c_i (Evans and Waugh, 1977*b*),

$$\frac{\Delta V}{V_0} = \frac{4\bar{T}}{\beta c_i}\left[\frac{\frac{A_p}{D_p} + \frac{A_c}{D_c}}{A_p + A_c}\right]. \tag{A1}$$

The isotropic tension, $\bar{T}$, is measured in dynes per centimeter; all dimensions are in centimeters; the concentration of solutes is in moles per liter; and the coefficient, β, ranges between $2.27–2.60 \times 10^7$ dyn-ℓ/mol · cm^2 for a temperature range of 10°–40°C. The areas and diameters for the vesicle projection inside and portion outside the pipet are given by (A_p, D_p) and (A_c, D_c) respectively. With Eq. A1 and typical experimental conditions (i.e., vesicle size, tension, salt concentration), the fractional change in volume is only ~0.001 and thus may be neglected in Eq. 1.

APPENDIX B

The beam compression test uses the deflection of a thin platinum beam as a force transducer. The force is proportional to displacement for small deflections. Since the vesicle volume is held fixed by the internal salt concentration, compression produces area dilation. Fig. A1 illustrates the micromanipulation. In the stepwise procedure, the vesicle is first aspirated with a small suction pressure, sufficient to form a spherical portion outside the pipet. The radius of the sphere is measured. Next the vesicle is compressed against the platinum beam. The beam displacement and equatorial radius of the vesicle are measured for several states of compression.

Since the vesicle geometry is specified by a surface of constant mean curvature (Evans and Skalak, 1979), the vesicle surface area and volume depend only on the equatorial radius, R_0, of the compressed capsule and the radius, R_i, of the contact with the flat surface,

$$V = R_0^3 f_v(\tilde{R})$$

and

$$A = R_0^2 f_a(\tilde{R}), \tag{A2}$$

where $\tilde{R}$ is the ratio R_i/R_0 of the contact radius to the equatorial radius. Hence, with the fixed internal volume, the dimensionless contact radius, $\tilde{R}$, is directly related to the equatorial radius. Also, the vesicle surface area becomes only a function of the equatorial radius. With the radius of the initially aspirated vesicle, we determine the surface area and volume of the spherical portion outside the pipet. The

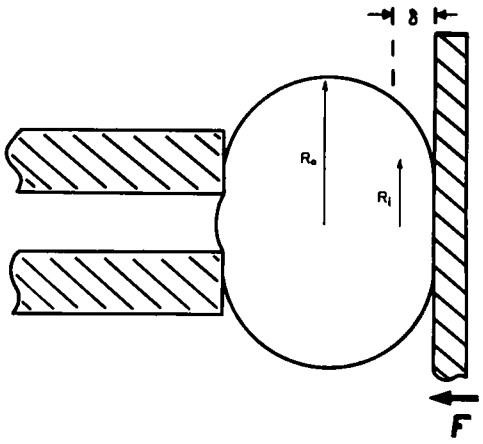

FIGURE A1 Schematic and cross-sectional shape that results from compression of a bilayer vesicle between a pipet and beam face. The beam force, F, is proportional to the displacement, δ. The geometry is specified by the fixed volume and equatorial radius, R_o. The radius R_i specifies the area of the flat contact with the beam face.

remainder of the vesicle inside the pipet is withdrawn by compression of the vesicle against the beam with a very small force. The equatorial radius of this "flattened" form is then used with the previous measurement of the spherical portion to determine the increase in area and volume due to the initial projection inside the pipet. The result is that the total surface area and volume of the vesicle are established for the unstressed state. This procedure defines an excess area fraction, α_0, which is the ratio of the initial (undeformed) area of the vesicle to the area of a sphere with the same volume minus one, i.e., $\alpha_0 = (A_0/A_s - 1)$. Surface area dilation due to temperature increase is evidenced as the increase in α_0 with temperature. Area dilation produced by forced compression of the vesicle against the beam is directly related to the increase in equatorial radius of the stressed vesicle. Fig. A1 illustrates the geometry of the compressed vesicle as a surface of constant mean curvature.

In the compression test, the beam force, F, is given by the excess pressure of the interior liquid relative to the exterior liquid multiplied by the area of contact.

$$F = \pi R_i^2 (P_c - P_0), \tag{A2}$$

where R_i is the radius of the contact area and $(P_c - P_0)$ is the pressure difference between the interior and exterior liquids, respectively. The balance of forces at the equator of the vesicle is used to relate the beam force to the membrane tension, $\overline{T}$.

$$F = \frac{2\pi R_i^2 R_0 \cdot \overline{T}}{(R_0^2 - R_i^2)} = \frac{2\pi \tilde{R}^2 R_0 \overline{T}}{(1 - \tilde{R}^2)}, \tag{A3}$$

where we have introduced the dimensionless contact radius, $\tilde{R}$. With the elastic constitutive relation, Eq. 3, the tension is related to the area dilation,

$$\overline{T} = \overline{T}_0 + K(A - A_0)/A_0, \tag{A4}$$

where A_0 and $\overline{T}_0$ are the values of vesicle surface area and membrane tension in the initial state. With the geometrical properties represented by Eq. A2 and the fixed volume, we see that Eqs. A3 and A4 combine to specify the beam force as a function of the initial tension, the area compressibility modulus, and the equatorial radius.

$$F = f(\overline{T}_0, K, R_0). \tag{A5}$$

Evans et al. (1980) used this relation and compression of an aspirated red blood cell against the platinum

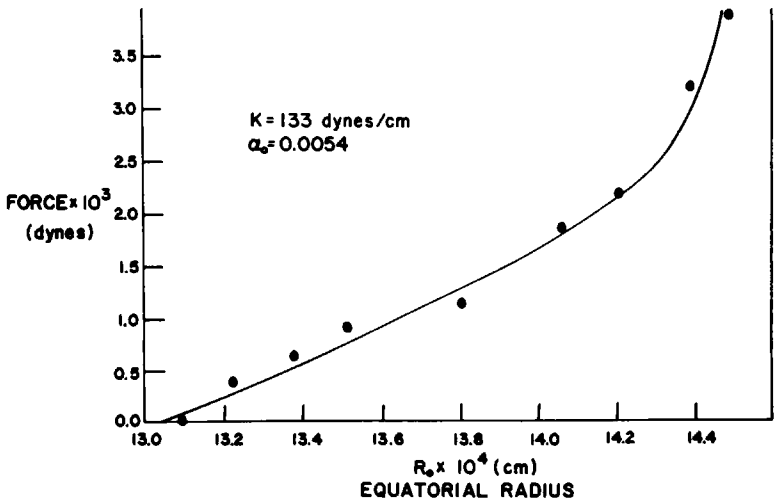

FIGURE A2 Data for beam force vs. the equatorial radius of a single-walled lecithin vesicle. The solid curve is the predicted behavior based on the area compressibility modulus of 133 dyn/cm. This vesicle possessed an initial excess area fraction (over that of a sphere of equal volume) given by $\alpha_o = 0.0054$.

beam to calibrate the beam force in terms of the displacement, δ.

$$F = k_B \cdot \delta. \tag{A6}$$

With this approach, the beam coefficient, k_B, can be determined for very thin beams, the minimum values being on the order of 0.1 dyn/cm. Thus, a micron of displacement is produced by 10^{-5} dyn (10 ng).

For vesicles which initially have excess area (over that of a sphere with the same volume), the initial tension is zero. Therefore, the beam displacement vs. the increase in equatorial radius (as the vesicle is compressed) provides the data of force as a function of equatorial radius. These data are then correlated with Eq. A5 and a specific value of the elastic area compressibility modulus. Fig. A2 shows data for a

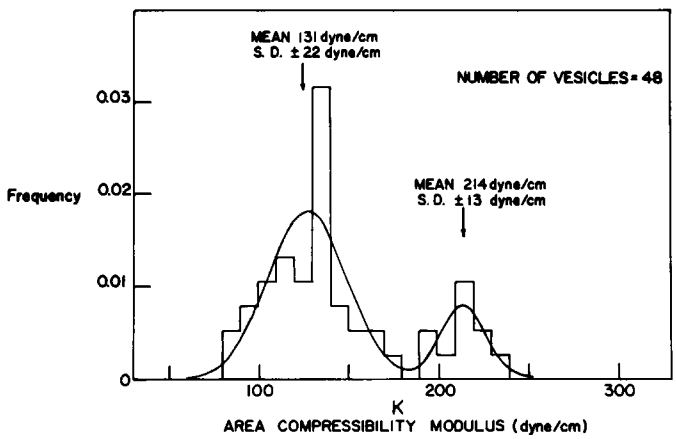

FIGURE A3 Histogram of elastic area compressibility moduli from the beam compression tests on large lecithin vesicles. The bimodal distribution separates the single-walled (lower elastic modulus) vesicles from the double-walled (higher modulus) vesicles. Two independent, normal distributions have been superimposed with the mean values and standard deviations of the data groups.

single vesicle compression test which has been correlated with Eq. A5 to determine the area compressibility modulus. The excess area fraction was determined by the procedure described above and is also given in Fig. A2.

The cumulated results for all vesicles tested by beam compression are shown in Fig. A3. Fig. A3 is the elastic area compressibility modulus histogram made up of moduli determined from force vs. equatorial radius data for 48 vesicles. The results are similar to those presented in Fig. 7. Likewise, the thermal area expansivity was calculated from excess area vs. temperature data and gave an average value of 2.6 $\times 10^{-3}$/°C.

APPENDIX C

When a vesicle is aspirated into a micropipet, the membrane must form a bend at the entrance to the pipet. Figure A4 is a schematic illustration of the membrane region that connects the aspirated projection with the exterior vesicle segment. The approximate scales are ~1 μm thickness for the pipet wall and 0.004 μm thickness for a bilayer membrane. Since the membrane is a very thin material, we expect the bend at the entrance to be relatively sharp. This means that the bending is essentially cylindrical (like the bending of a flat sheet around a corner). Therefore, the principal curvature, $\partial\theta/\partial s$, along the curvilinear direction, s, is much greater than the other principal curvature, $\sin\theta/r$, which is derived in the plane normal to the direction, s. Along with the curvilinear coordinates, s and θ, the membrane force resultants are shown in Fig. A4, where $\bar{T}$ is the membrane tension and Q_T is the transverse shear produced by bending the membrane. The transverse shear is the derivative of the membrane bending moment, M:

$$Q_T = \frac{dM}{ds}. \tag{A7}$$

Mechanical equilibrium may be represented by the balance of forces tangent to the surface, which yields:

$$\frac{d\bar{T}}{ds} + \frac{d\theta}{ds} \cdot Q_T = 0, \tag{A8}$$

and the balance of forces parallel to the pipet axis which yields one equation for outside the pipet:

$$\frac{r(P_c - P_0)}{2} = \bar{T} \cdot \sin\theta - Q_T \cdot \cos\theta, \tag{A9}$$

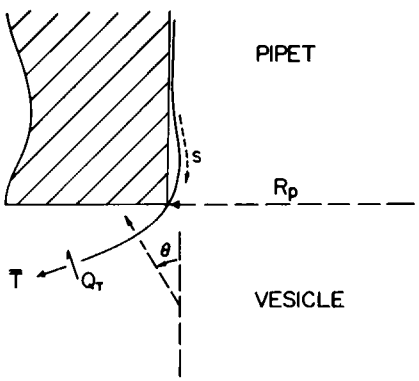

FIGURE A4 Schematic of the membrane bend and edge contact at the pipet entrance. The force resultants involved in membrane equilibrium are the tension, $\bar{T}$, and transverse shear, Q_T, produced by bending.

and another equation for inside the pipet:

$$\frac{r(P_c - P_p)}{2} = \bar{T} \cdot \sin\theta - Q_T \cdot \cos\theta, \tag{A10}$$

where r is the radial distance from the axis of symmetry to the membrane and P_p, P_c, P_0 are the pressures inside the pipet, inside the vesicle, and outside the vesicle, respectively (Evans and Skalak, 1979). We see that axial forces are not continuous at the edge contact with the glass pipet. At the edge contact, there is a load applied to the membrane created by the net force from the pipet suction, $\Delta P(\pi R_p^2)$. This load is balanced by a discontinuity in transverse shear:

$$\frac{R_p \cdot \Delta P}{2} = \cos\theta_e (Q_T^+ - Q_T^-), \tag{A11}$$

where Q_T^+ and Q_T^- are the values of transverse shear near the edge contact approached from outside and inside the pipet, respectively and θ_e is the value of the membrane angle at the edge contact. Since the transverse shear is the spatial derivative of the bending moment, the next axial force is given by a discontinuity in the derivative of the bending moment:

$$\frac{\Delta P \cdot R_p}{2} = \cos\theta_e \left(\frac{dM^+}{ds} - \frac{dM^-}{ds}\right). \tag{A12}$$

The bending moment is determined from an elastic constitutive relation. The first order equation for cylindrical bending is a simple proportionality between the bending moment and the membrane curvature (Evans and Skalak, 1979),

$$M = B \cdot \frac{d\theta}{ds}, \tag{A13}$$

where B is the elastic bending modulus.

For a sharp bend, the solutions to Eqs. A8, A9, and A10 are given by:

$$\begin{aligned} \bar{T} &= C_p \cdot \sin\theta + C_I \cdot \cos\theta, \\ Q_T &= -C_p \cdot \cos\theta + C_I \cdot \sin\theta, \end{aligned} \tag{A14}$$

where the coefficient C_p is $R_p (P_c - P_0)/2$ outside the pipet and $R_p (P_c - P_p)/2$ inside the pipet; the coefficient C_I depends on the boundary conditions.

With the elastic constitutive relation (Eq. A13) and the equilibrium equation (Eq. A8), the tension is determined as a function of curvature along the surface contour.

$$\bar{T} = C_T - \frac{B}{2}\left(\frac{d\theta}{ds}\right)^2 \tag{A15}$$

where C_T is the uniform tension in regions where the curvature is negligible (i.e., away from the sharp bend). Thus, the tension is continuous along the contour but its derivative is discontinuous at the edge contact, $\theta = \theta_e$, as confirmed by Eqs. A8, A11, and A14.

Since the pressure difference $(P_c - P_0)$ is much less than $(P_c - P_p)$, the $\cos\theta_e$ is very small and Eqs. A14 and A15 combine to provide an estimate of the proportionality of the suction pressure, ΔP, to the curvature at the edge contact, $1/R_c$:

$$\Delta P = \sim\frac{2B}{D_p}\left(\frac{1}{R_c}\right)^2$$

where D_p is the pipet diameter and R_c is the radius of curvature of the sharp bend.

This work was supported in part by U.S. Public Health Service/National Institutes of Health grants HL 16711 and HL 26965.

Received for publication 2 January 1981 and in revised form 1 May 1981.

REFERENCES

Alvarez, O., and R. Latorre. 1978. Voltage-dependent capacitance in lipid bilayers made from monolayers. *Biophys. J.* 21:1–17.

Crowley, J. M. 1973. Electrical breakdown of bimolecular lipid membranes as an electromechanical instability. *Biophys. J.* 13:711–724.

Elworthy, P. H. 1961. The adsorption of water vapor by lecithin and lysolecithin, and the hydration of lysolecithin micelles. *J. Chem. Soc. (Lond.).* 5385–5389.

Evans, E. A., and R. M. Hochmuth. 1978. Mechanochemical properties of membranes. *Curr. Top. Membr. Transp.* 10:1–64.

Evans, E. A., R. Kwok, and J. T. McCown. 1980. Calibration of beam deflection produced by cellular forces in the 10^{-9}–10^{-6} gram range. *Cell Biophys.* 2:99–112.

Evans, E. A., and R. Skalak. 1979. Mechanics and thermodynamics of biomembranes. *Crit. Rev. Bioeng.* 3 and 4: 181–418. (1980. Monograph. C. R. C. Press. Boca Raton, Fla.).

Evans, E. A., and R. Waugh. 1977a. Mechano-chemistry of closed, vesicular membrane systems. *J. Colloid Interface Sci.* 60:286–298.

Evans, E. A., and R. Waugh. 1977b. Osmotic correction to elastic area compressibility measurements on red cell membrane. *Biophys. J.* 20:307–313.

Evans, E. A., R. Waugh, and L. Melnik. 1976. Elastic area compressibility modulus of red cell membrane. *Biophys. J.* 16:585–595.

Kwok, R. 1980. Thermoelasticity of large phospholipid bilayer vesicles. Dissertation, Duke University, Durham, N.C.

LeNeveu, D. M., R. P. Rand, V. A. Parsegian, and D. Gingell. 1977. Measurement and modification of forces between lecithin bilayers. *Biophys. J.* 18:209–230.

Liu, N.-I., and R. L. Kay. 1977. Redetermination of the pressure dependence of the lipid bilayer phase transition. *Biochemistry.* 16:3484–3486.

McDonald, A. G. 1978. A dilatometric investigation of the effects of general anaesthetics, alcohols, and hydrostatic pressure on the phase transition in smectic mesophases of dipalmitoyl phosphatidylcholine. *Biochim. Biophys. Acta.* 507:26–37.

Montal, M., and P. Mueller. 1972. Formation of bimolecular membranes from lipid monolayers and a study of their electrical properties. *Proc. Natl. Acad. Sci. U. S. A.* 69:3561–3566.

Nagle, J. F., and D. A. Wilkinson. 1978. Lecithin bilayers: Density measurements and molecular interactions. *Biophys. J.* 23:159–175.

Pagano, R. E., and T. E. Thompson. 1973. Spherical lipid bilayers: surface tension and contact angle measurements. *J. Colloid Interface Sci.* 43:209–210.

Parsegian, V. A., N. Fuller, and R. P. Rand. 1979. Measured work of deformation and repulsion of lecithin bilayers. *Proc. Natl. Acad. Sci. U. S. A.* 76:2750–2754.

Rand, R. P., and W. A. Pangborn. 1973. A structural transition in egg lecithin-cholesterol bilayers at 12°C. *Biochim. Biophys. Acta.* 318:299–305.

Reeves, J. P., and R. M. Dowben. 1969. Formation and properties of thin-walled phospholipid vesicles. *J. Cell. Physiol.* 73:49–60.

Requena, J., D. A. Haydon, and S. B. Hladky. 1975. Lenses and the compression of black lipid membranes by an electric field. *Biophys. J.* 15:77–81.

Reiss-Husson, F. 1967. Structure des phases liquide-cristallines de différents phospholipids, monoglycerides, sphingolipides, anhydres, ou en présence d'eau. *J. Mol. Biol.* 25:363–382.

Tien, H. T. 1967. Black lipid membranes in aqueous media: interfacial free energy measurements and effect of surfactants on film formation and stability. *J. Phys. Chem.* 71:3395–3401.

White, S. H., and T. E. Thompson. 1973. Capacitance, area, and thickness variation in thin lipid films. *Biochim. Biophys. Acta.* 323:7–22.

Waugh, R., and E. A. Evans. 1979. Thermoelasticity of red blood cell membrane. *Biophys. J.* 26:115–132.